Check for updates

Mycobacterium tuberculosis EspK Has Active but Distinct Roles in the Secretion of EsxA and EspB

Ze Long Lim,[a] Kylee Drever,[a,b] Neeraj Dhar,[a,c] (ID)Stewart T. Cole,[d] (ID)Jeffrey M. Chen[a,b]

[a]Vaccine and Infectious Disease Organization, Saskatoon, Canada
[b]Department of Veterinary Microbiology, Western College of Veterinary Medicine, University of Saskatchewan, Saskatoon, Canada
[c]École Polytechnique Fédérale de Lausanne, Global Health Institute, Lausanne, Switzerland
[d]Institut Pasteur, Paris, France

ABSTRACT The *Mycobacterium tuberculosis* type-7 protein secretion system ESX-1 is a major driver of its virulence. While the functions of most ESX-1 components are characterized, many others remain poorly defined. In this study, we examined the role of EspK, an ESX-1-associated protein that is thought to be dispensable for ESX-1 activity in members of the *Mycobacterium tuberculosis* complex. We show that EspK is needed for the timely and optimal secretion of EsxA and absolutely essential for EspB secretion in *M. tuberculosis* Erdman. We demonstrate that only the EsxA secretion defect can be alleviated in EspK-deficient *M. tuberculosis* by culturing it in media containing detergents like Tween 80 or tyloxapol. Subcellular fractionation experiments reveal EspK is exported by *M. tuberculosis* in an ESX-1-independent manner and localized to its cell wall. We also show a conserved W-X-G motif in EspK is important for its interaction with EspB and enabling its secretion. The same motif, however, is not important for EspK localization in the cell wall. Finally, we show EspB in EspK-deficient *M. tuberculosis* tends to adopt higher-order oligomeric conformations, more so than EspB in wild-type *M. tuberculosis*. These results suggest EspK interacts with EspB and prevents it from assembling prematurely into macromolecular complexes that are presumably too large to pass through the membrane-spanning ESX-1 translocon assembly. Collectively, our findings indicate *M. tuberculosis* EspK has a far more active role in ESX-1-mediated secretion than was previously appreciated and underscores the complex nature of this secretion apparatus.

IMPORTANCE *Mycobacterium tuberculosis* uses its ESX-1 system to secrete EsxA and EspB into a host to cause disease. We show that EspK, a protein whose role in the ESX-1 machinery was thought to be nonessential, is needed by *M. tuberculosis* for optimal EsxA and EspB secretion. Culturing EspK-deficient *M. tuberculosis* with detergents alleviates EsxA but not EspB secretion defects. We also show that EspK, which is exported by *M. tuberculosis* in an ESX-1-independent manner to the cell wall, interacts with and prevents EspB from assembling into large structures inside the *M. tuberculosis* cell that are nonsecretable. Collectively, our observations demonstrate EspK is an active component of the ESX-1 secretion machinery of the tubercle bacillus.

KEYWORDS *Mycobacterium tuberculosis*, ESX-1, EspK, protein secretion, virulence

The multiprotein type-7 protein secretion system ESX-1, which is used to translocate the virulence effector proteins EsxA, EsxB, EspA, EspB, and EspC, is encoded by genes in the *esx-1* locus and *espACD* operon (1). ESX-1 protein components are highly conserved in members of the *Mycobacterium tuberculosis* complex (MTBC), like *M. tuberculosis*, *M. bovis*, and *M. africanum*, as well as in nontuberculous pathogenic mycobacteria, like *M. marinum*, *M. kansasii*, and *M. leprae* (1). From a combination of different structural studies of type-7 ESX systems (2–5), it is predicted that the cytoplasmic membrane-spanning section of ESX-1

is an oligomeric structure with 6-fold symmetry composed of five conserved proteins, $EccB_1$, $EccCa_1$, $EccCb_1$, $EccD_1$, and $EccE_1$. Heterodimers of Esx or Esp substrate proteins, each bearing a conserved Y-X-X-X-D/E or W-X-G motif, are proposed to pass through this channel (4). One such substrate protein, EspB, is expressed as a 60-kDa protein, but during its translocation it gets truncated at its carboxy terminus to a 50-kDa secreted isoform by a serine protease domain in the periplasmic part of the membrane-associated $MycP_1$ protein (6). Once outside the *M. tuberculosis* cell, EspB forms a heptameric ring-shaped structure that has a distinct virulence function and is speculated to also be involved in ESX-1 secretion activity (7–11). While the precise roles of most ESX-1-associated proteins have been defined, the function and spatiotemporal organization of some remain unclear.

EspK is a 75-kDa alanine- and proline-rich ESX-1-associated protein with a conserved W-X-G motif. In *M. tuberculosis*, EspK is encoded by the *espK* (*rv3879c*) gene in the *esx-1* locus (1, 12–14). Deletion of the *espK* homolog in *M. bovis* does not impair its ability to replicate in the lungs and spleen or cause lesions in the lymphoid organs of guinea pigs (15). The effect of EspK deficiency on *M. bovis* ESX-1 secretion activity, however, is not known (15). Complementation of the live, attenuated, and ESX-1-deficient *M. bovis* BCG vaccine strain with either the complete *esx-1* locus or a modified *esx-1* locus lacking *espK* restores EsxA and EsxB secretion and increases its virulence in mice equally, suggesting EspK is not required for ESX-1 function (12). Furthermore, *M. africanum*, which causes 50% of the pulmonary tuberculosis cases in West Africa, is EspK deficient due to a premature stop codon mutation in its *espK* gene (16). Despite lacking EspK, *M. africanum* can secrete EsxA and EsxB (16). Interestingly, however, *M. africanum* has been shown to not replicate as well and induce as much pathology in mice as *M. tuberculosis*, although this has been attributed to its longer cell length and lack of EspK (16, 17). *M. marinum*, the causative agent of TB in cold-blooded vertebrates, skin infections in humans, and a valuable mycobacterial surrogate for studying the ESX-1 system, possesses two orthologs of EspK encoded by MMAR_5455 and MMAR_4351 (18, 19). Notably, EspK, encoded by MMAR_5455, is translocated from the *M. marinum* cytosol to the capsular layer (20) and extracellular milieu in an ESX-1-dependent manner (21, 22). EspK-deficient *M. marinum* exhibits diminished EsxA and EsxB secretion but not at levels seen in isogenic $EccCb_1$- or $EccD_1$-deficient mutants as well as the complete blockage of EspB secretion (22). In another study, however, an EspK-deficient *M. marinum* strain was found to be defective in EsxA but not EsxB secretion, impaired in its ability to replicate in murine bone marrow-derived macrophages (BMDMs) and in killing J774 macrophages (23). In a different study, *M. marinum* deficient in EspK was found to secrete EsxB but not EspB and was compromised in its ability to replicate in BMDMs (24). In the same study, EspK was shown to interact with EspB and $EccCb_1$, an ESX-1 core component, presumably to direct EspB to the ESX-1 secretion machinery for transport out of the *M. marinum* cell (24). In yet another study, EspK deficiency in *M. marinum* was found to reduce EsxA but not EsxB secretion, cause some attenuation of virulence, and diminish the induction of type I interferon responses in macrophages (25). Despite extensive downsizing of its genome, *M. leprae*, the obligate intracellular pathogen and agent of leprosy, has retained an ESX-1 system whose secretion activity is likely functional (26–29). However, in *M. leprae espK* is a pseudogene, suggesting it is dispensable for its ESX-1 system (13).

Given the inconsistencies in phenotypes associated with EspK deficiency among pathogenic mycobacteria, the biological role of this ESX-1-associated protein in *M. tuberculosis* remains uncertain. Here, we characterize an *espK* transposon insertion mutant of *M. tuberculosis* Erdman and present compelling evidence to show that EspK plays an active and multifaceted role in driving optimal ESX-1-mediated protein secretion.

RESULTS

EspK deficiency in *M. tuberculosis* impacts EsxA and EspB secretion but not its cytopathic potential or ability to replicate in mice. An *M. tuberculosis espK* transposon mutant (*espK*::Tn) strain was isolated from a previously archived library of *M. tuberculosis* Erdman Tn*5370* transposon mutants (30). Genome sequencing revealed that Tn*5370*,

bearing a hygromycin resistance cassette, had inserted 295 bp downstream of the start codon of *espK* in this mutant strain (Fig. 1A).

Having confirmed wild-type (WT) *M. tuberculosis* Erdman and *espK*::Tn strains replicate at similar rates in mycobacterial liquid growth media like Middlebrook 7H9 and Sauton's media (Fig. 1B), we examined the impact of *espK* disruption on ESX-1-mediated protein secretion. Accordingly, WT *M. tuberculosis*, *espK*::Tn, and a well-characterized isogenic 5′ Tn::*pe35* strain that fails to express EsxA and EsxB, and consequently lacking ESX-1 secretion activity (7, 31, 32), were cultured in detergent-free Sauton's medium for 3 days. The culture filtrate (CF) and cell lysate (CL) fractions of these strains were then assessed for EsxA, EsxB, EspB, and EspK proteins. EspK was detected only in the CL of WT *M. tuberculosis* and 5′ Tn::*pe35* strains, which suggests this protein is primarily cell associated (Fig. 1C). As expected, EspK was not detected in either the CF or CL fractions of the *espK*::Tn strain (Fig. 1C). Interestingly, the amount of EspK in the CL of the 5′ Tn::*pe35* strain appeared to be 8% less than that of WT *M. tuberculosis* (Fig. 1C), which is consistent with what has been reported for EspK in a *M. marinum* Δ*esxAB* mutant strain compared to its WT counterpart (22). Compared to WT *M. tuberculosis*, 30% less EsxA and no EspB (50-kDa secreted isoform) were detected in the CF of the *espK*::Tn strain (Fig. 1C). In contrast, similar amounts of EsxB were detected in the CF of both WT *M. tuberculosis* and the *espK*::Tn strain (Fig. 1C). Equivalent amounts of EsxA, EsxB, and EspB (full-length 60-kDa isoform) were detected in the CL fractions of both WT *M. tuberculosis* and *espK*::Tn strains, indicating equivalent expression and/or stability of these proteins in the two strains (Fig. 1C). Consistent with our previous reports (7, 31, 32), EsxA, EsxB, and EspB (50 kDa) were not detected in the CF, while EspB only was detected in the CL of the 5′ Tn::*pe35* strain (Fig. 1C).

To confirm equivalent amounts of CF proteins from all three strains were loaded and analyzed, we immunoblotted for antigen-85 (Ag85), which is secreted by *M. tuberculosis* in an ESX-1-independent manner via the twin arginine transport (TAT) system (33). Similar amounts of this protein were found in the CF of all three strains, indicating that the differences in the levels of EsxA and EspB were not due to uneven protein loading. Finally, to verify that the presence of specific proteins in the CF was not due to cell lysis, we immunoblotted for the cell-associated chaperonin GroEL2 (34). No GroEL2 was detected in the CF of WT *M. tuberculosis*, *espK*::Tn, and 5′ Tn::*pe35* strains. In contrast, similar amounts of GroEL2 were detected in the CL of the three strains. This indicated that the differences in the levels of EsxA and EspB were not due to cell lysis and that equivalent amounts of total CL protein from the three strains had been loaded and analyzed.

We had previously reported that WT *M. tuberculosis* induces cell death in macrophages and replicates in the lungs and spleens of mice in an ESX-1-dependent manner (7, 32, 35). Given the secretion defects noted above, we expected the *espK*::Tn strain to be compromised in these functions as well. To test this, THP-1 cells were infected with WT *M. tuberculosis*, the *espK*::Tn strain, and an attenuated *espA*::Tn mutant strain that is defective in EsxA and EsxB but not EspB secretion (7). Death induced by these *M. tuberculosis* strains in THP-1 cells was then assessed. Unlike the *espA*::Tn strain, the *espK*::Tn strain induced the same magnitude of cell death in THP-1 cells as WT *M. tuberculosis* (Fig. 1D). To examine *in vivo* replication, mice were infected by the aerosol route with WT *M. tuberculosis* and the *espK*::Tn strain. Bacterial burden in the lungs and spleens were enumerated after 3 and 6 weeks postchallenge. Consistent with the macrophage cell death results, the *espK*::Tn strain appeared to replicate as well as WT *M. tuberculosis* in the lungs and spleens of mice (Fig. 1E).

These results show EspK deficiency in *M. tuberculosis* causes unique defects in EsxA and EspB secretion *in vitro* but does not seem to impact the bacterium's ability to induce macrophage cell death or replicate in mice.

M. tuberculosis exports EspK across its cytoplasmic membrane in an ESX-1-independent manner to the cell wall. *M. marinum* exports EspK to its capsule (20) and into the extracellular milieu in an ESX-1-dependent manner (21, 22). Although we did not detect EspK in 10 μg of total CF protein from WT *M. tuberculosis* (Fig. 1C), we
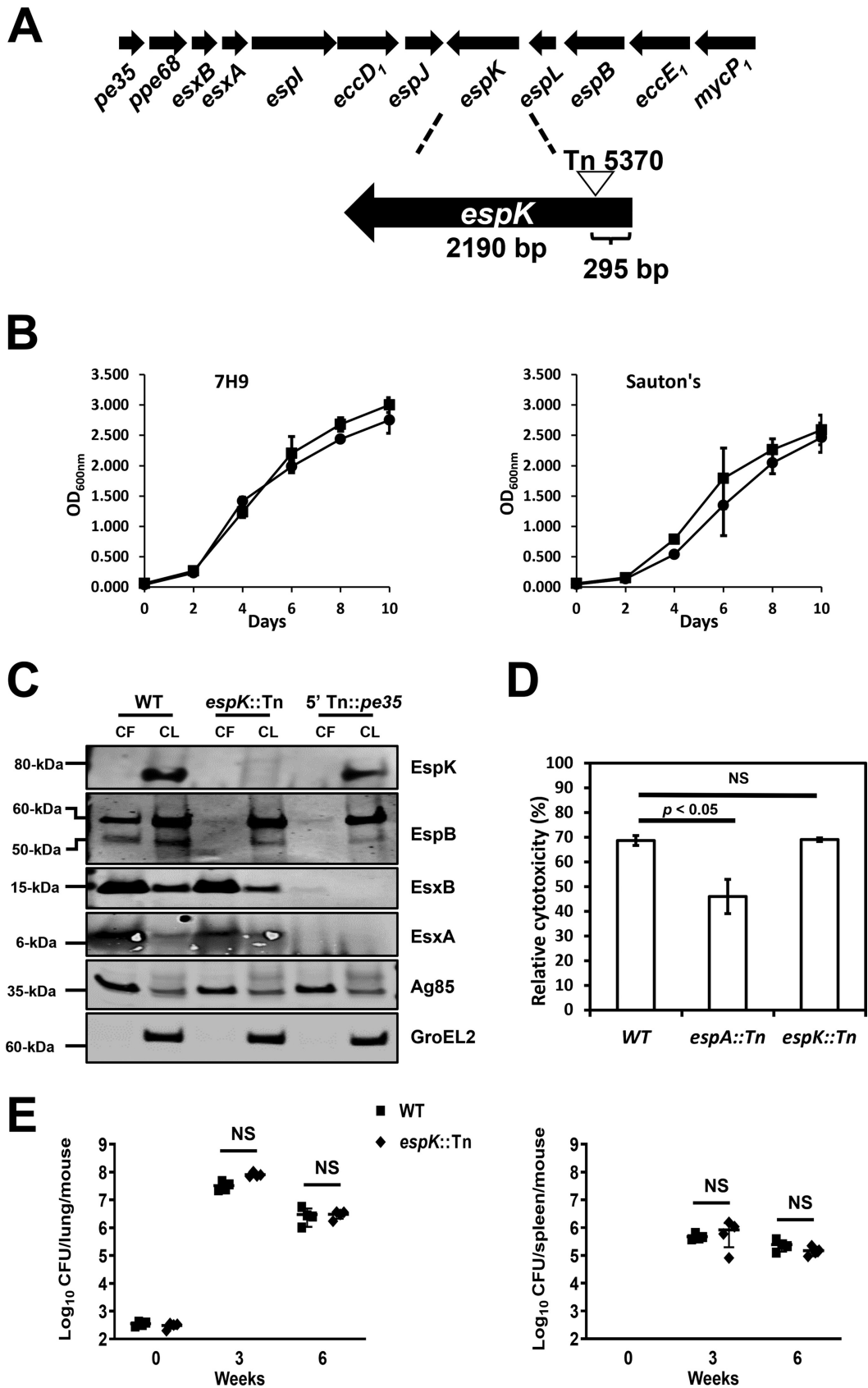
FIG 1 Characterization of the *M. tuberculosis espK*::Tn mutant. (A) Schematic of transposon insertion into the *espK* gene in the *esx-1* locus of *M. tuberculosis* Erdman. (B) Growth comparison of wild-type *M. tuberculosis* Erdman (WT) and isogenic *espK*::Tn
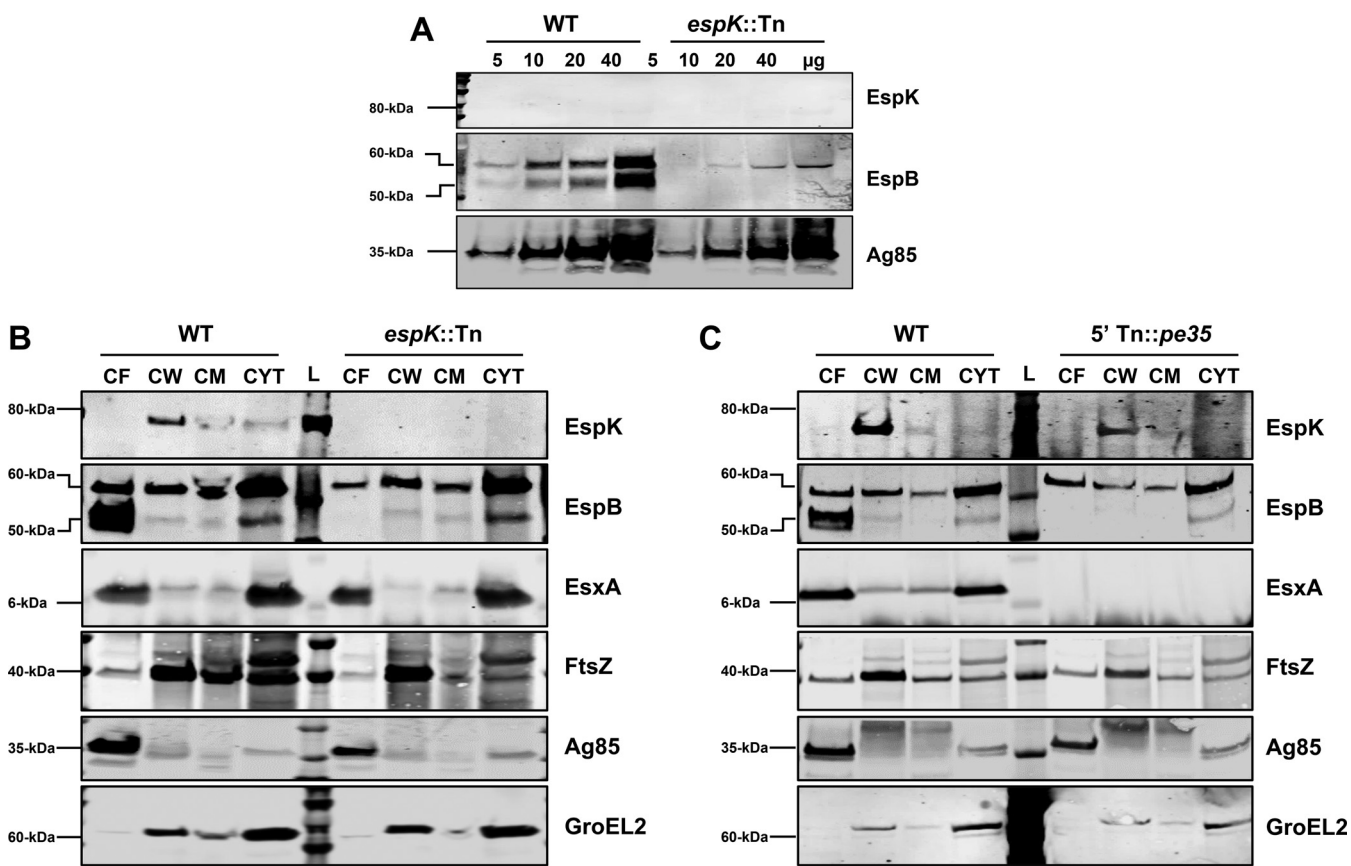
FIG 2 Cellular localization of EspK in *M. tuberculosis* Erdman strains. (A to C) Immunoblots of increasing amounts of total CF protein of wild-type *M. tuberculosis* Erdman (WT) versus *espK*::Tn mutant strain (A), 10 μg/well each of CF, CW, CM, and cytosol proteins from wild-type *M. tuberculosis* Erdman (WT) versus *espK*::Tn strain (B), and wild-type *M. tuberculosis* Erdman (WT) versus 5′ Tn::*pe35* strain (C) (each set of blots is representative of at least 2 independent experiments; L, protein ladder).

could not discount the possibility that the protein is present at very low levels. To address this, increasing amounts of WT *M. tuberculosis* CF starting from 5 to 40 μg of total protein was examined. Despite numerous attempts, EspK was not detected in the CFs of both the WT *M. tuberculosis* and the *espK*::Tn strain (Fig. 2A). EspB (50 kDa), on the other hand, was found at increasing amounts in the CFs of WT *M. tuberculosis* but undetectable in the CFs of the *espK*::Tn strain (Fig. 2A). Increasing amounts of Ag85 were detected in the CFs of both the WT *M. tuberculosis* and *espK*::Tn strains, indicating the differential detection of EspB was not due to uneven loading of protein samples in the gel (Fig. 2A).

We next examined if EspK might still be exported by WT *M. tuberculosis* across its cytoplasmic membrane (CM) and localized to the cell surface. Accordingly, subcellular fractions namely, the cell wall (CW), CM, and cytosol of WT *M. tuberculosis*, *espK*::Tn, and 5′Tn::*pe35* strains were prepared using established methods (36–38). These, along with their respective CF fractions, were analyzed by immunoblotting. Consistent with previous reports

FIG 1 Legend (Continued)

mutant strain in 7H9 (left) and Sauton's (right) medium (average of 2 independent experiments; error bars represent the standard deviations). (C) Immunoblots of CF (10 μg/well) and CL total protein (5 μg/well) of wild-type *M. tuberculosis* Erdman (WT), *espK*::Tn, and 5′ Tn::*pe35* strains cultured 3 days in Sauton's medium without detergent to examine indicated proteins (representative of 3 independent experiments). (D) Cytotoxicity assay in THP-1 cells infected with wild-type *M. tuberculosis* Erdman (WT), *espA*::Tn, and *espK*::Tn strains at an MOI of 5 (data represent means and standard errors of means from 4 independent experiments with replicate wells; the *y* axis indicates cytotoxicity values relative to uninfected control; significance in difference calculated using Student's *t* test). (E) Bacterial burden after 3 and 6 weeks postinfection in lungs (top) and spleens (bottom) of mouse aerosol challenged with wild-type *M. tuberculosis* Erdman (WT) and *espK*::Tn strain (each data point indicates the bacterial burden per mouse, with median and standard deviations from 4 mice per group per time point shown; significance in difference calculated using Student's *t* test; NS, not significant).

(34, 39), FtsZ, a cell division protein, was detected primarily in the CW fraction and, to a lesser degree, in the CF, CM, and cytosol fractions, while the cell-associated chaperonin GroEL2 was found in the CW and cytosol fractions of all three *M. tuberculosis* strains (Fig. 2B and C). These results confirmed successful ultracentrifugation-mediated fractionation of the CL and enrichment of specific proteins in their cellular locations. As expected, EsxA was detected primarily in the CF and cytosol of both the WT *M. tuberculosis* and *espK*::Tn strains, while secreted EspB (50-kDa) was found predominantly in the CF of WT *M. tuberculosis* only (Fig. 2B and C). Also as expected, large amounts of full-length EspB (60 kDa) were detected in the cytosol of the WT *M. tuberculosis*, *espK*::Tn, and 5′Tn::*pe35* strains (Fig. 2B and C). Interestingly, EspK was detected primarily in the CW of both WT *M. tuberculosis* and 5′Tn::*pe35* strains (Fig. 2B and C) but not in any of the subcellular fractions of the *espK*::Tn strain (Fig. 2B). Detection of EspK in the CW fraction of WT *M. tuberculosis* H37Rv confirmed enrichment of this protein in the cell wall is not unique to *M. tuberculosis* Erdman (see Fig. S1 in the supplemental material).

These results suggest EspK is localized in the *M. tuberculosis* cell wall compartment and unlike EsxA, EsxB, or EspB, it is not released into the extracellular milieu. Furthermore, the localization of EspK in the cell wall of the 5′Tn::*pe35* strain suggests it crosses the *M. tuberculosis* cytoplasmic membrane in an EsxA- and EsxB-independent manner.

EspK deficiency delays and reduces EsxA secretion. In this study, multiple independent sets of CF preparations from 3-day-old cultures of WT *M. tuberculosis* and *espK*::Tn strains were analyzed. In most instances, reduced levels of EsxA were detected in the CF of the *espK*::Tn strain compared to WT *M. tuberculosis*. EspB, on the other hand, was always absent from the CF of the mutant strain. We therefore asked if EspK deficiency might be delaying the secretion of EsxA and potentially also of EspB. To address this question, the CF and CL of WT *M. tuberculosis* and *espK*::Tn strains cultured for 3, 5, and 7 days in Sauton's medium were analyzed. While the levels of EsxA and EsxB in the CFs of WT *M. tuberculosis* collected after 3, 5, and 7 days of culturing appeared to be similar, the level of EsxA in the CF of the *espK*::Tn strain, which was lower than that of WT *M. tuberculosis* on day 3, increased with time (Fig. 3A). By day 5, for instance, the amount of EsxA detected in the CF of the *espK*::Tn strain had increased to 80% of the EsxA in the CF of WT *M. tuberculosis*. By day 7, the amount of EsxA in the CF of the *espK*::Tn strain had increased to 85% of the EsxA in the CF of WT *M. tuberculosis*. The levels of EsxB, on the other hand, did not appear to change significantly in the CF of the *espK*::Tn strain collected at the three time points (Fig. 3A). In stark contrast, no EspB (50 kDa) could be detected in the CF of the *espK*::Tn strain even by 7 days of growth, while the level of EspB (50 kDa) was somewhat constant in the CF of WT *M. tuberculosis* collected over the three time points (Fig. 3A).

To exclude the possibility that delayed secretion in *espK*::Tn strain might be unique to Sauton's medium, the CF and CL fractions of WT *M. tuberculosis* and the *espK*::Tn strain grown for 3, 5, and 7 days in modified 7H9 medium (without ADC and Tween 80) were also analyzed. A pattern similar to what was seen in Sauton's medium was also observed with 7H9. While EsxA in the CFs of WT *M. tuberculosis* appeared relatively constant over the three time points, the level of EsxA in the CF of the *espK*::Tn strain, which was lower than that of WT *M. tuberculosis* on day 3, appeared to increase with time (Fig. 3B). By day 5, the amount of EsxA detected in the CF of the *espK*::Tn strain had increased to 92% of the level of EsxA in the CF of WT *M. tuberculosis*. By day 7, the amount of EsxA in the *espK*::Tn CF had reached to 97% of the EsxA level in the CF of WT *M. tuberculosis*. Likewise, no EspB (50 kDa) was detected in the CF of the *espK*::Tn strain even after 7 days of growth, while the levels of EspB appeared constant over the three time points (Fig. 3B).

These results indicate that EspK deficiency in *M. tuberculosis* causes delayed and somewhat reduced EsxA secretion, while the secretion of EspB is completely blocked. Moreover, this unique secretion defect is independent of the type of culture medium used to grow the bacteria.
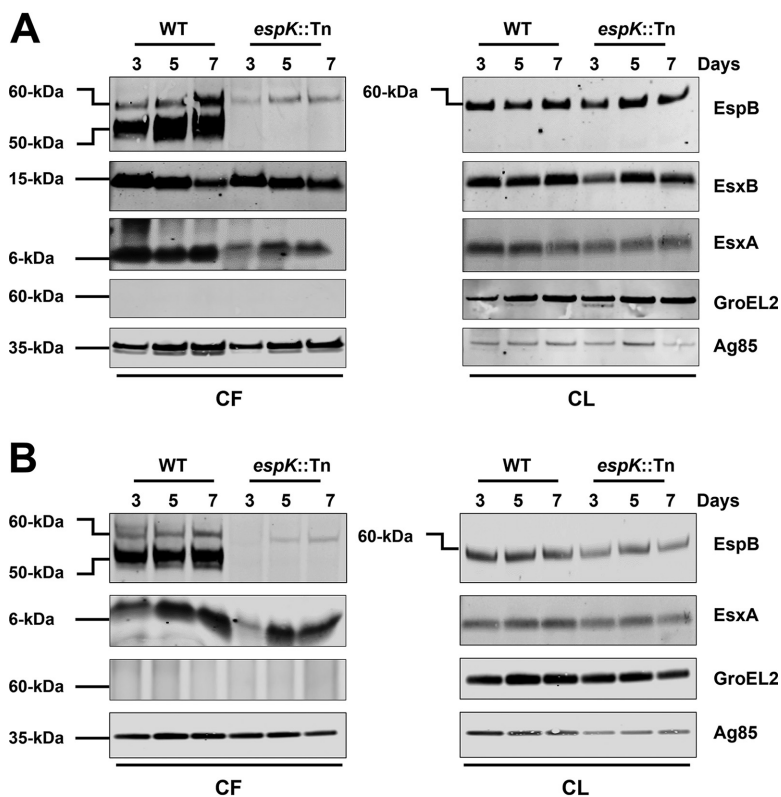
FIG 3 Secretion and expression of ESX-1-associated proteins in liquid culture media over time. Immunoblots of CF (10 μg/well) and CL proteins (5 μg/well) of wild-type *M. tuberculosis* Erdman (WT) and *espK*::Tn mutant cultured 3, 5, and 7 days in Sauton's medium without detergent (A) and modified 7H9 medium without ADC and detergent supplementation (B) (each set of blots is representative of 3 independent experiments).

Faulty EsxA secretion in EspK-deficient *M. tuberculosis* can be partially restored to WT *M. tuberculosis* levels by culturing in detergent-containing media. To understand why the *espK*::Tn strain, despite its secretion defects, is not compromised in its ability to induce macrophage cell death or replicate in mice, we reexamined the published research on EspK-deficient *M. bovis* BCG and *M. africanum* (12, 15, 16) and our own procedures. We realized that mycobacteria are always grown in detergent-containing media to reduce cell clumping and obtain single-cell suspensions prior to use in infections. We therefore hypothesized that culturing the *espK*::Tn strain with detergents might alleviate its ESX-1 secretion defects and explain the unimpaired virulence observed. To test this, WT *M. tuberculosis* and the *espK*::Tn mutant were cultured in Sauton's medium supplemented with or without 0.05% Tween 80 for 3 days and their CF and CL proteins analyzed. We detected an 8-fold increase in the levels of EsxA in the CF of *espK*::Tn cultured in Sauton's with Tween 80 compared to Sauton's without detergent (Fig. 4A). We also observed the level of EsxA in the CF of *espK*::Tn cultured with Tween 80 was 1.5-fold more than that of WT *M. tuberculosis* grown without detergent. In contrast, no EspB (50 kDa) was detected in the CF of *espK*::Tn grown with and without Tween 80 (Fig. 4A). Moreover, 5-fold more EsxA was detected in the CF of WT *M. tuberculosis* cultured in Sauton's with Tween 80 compared to media without detergent (Fig. 4A). In contrast, EsxB levels were similar regardless of whether or not Tween 80 was present. We found EspB (50 kDa) levels in the CF of WT *M. tuberculosis* cultured with Tween 80 decreased by 40% relative to EspB levels in the CF of WT *M. tuberculosis* cultured without the detergent (Fig. 4A).

To exclude the possibility that enhancement of EsxA secretion is unique to Tween 80, WT *M. tuberculosis* and the *espK*::Tn strain were also cultured for 3 days in Sauton's medium with 0.02% tyloxapol, another detergent that is used to prevent mycobacterial
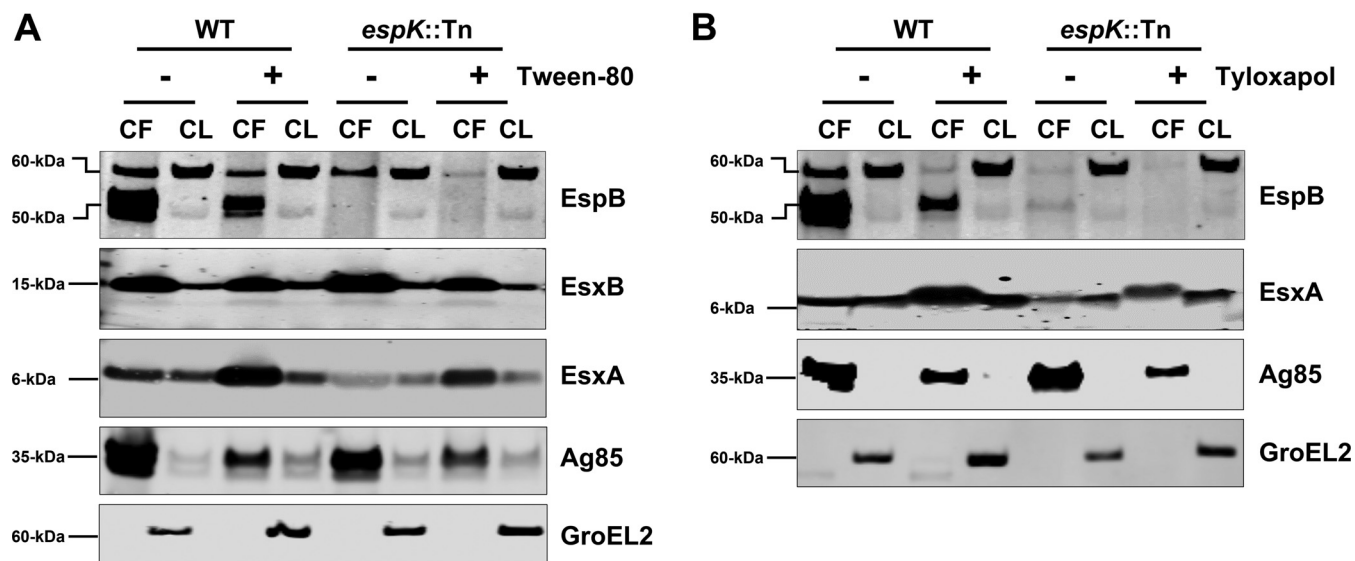
FIG 4 Secretion and expression of ESX-1 associated proteins in WT *M. tuberculosis* and *espK*::Tn cultured in liquid media with and without detergents. (A and B) Immunoblots of CF (10 µg/well) and CL (5 µg/well) total protein of wild-type *M. tuberculosis* Erdman (WT) and *espK*::Tn mutant cultured for 3 days in Sauton's medium with and without Tween 80 (A) and Sauton's medium with and without tyloxapol (B) to examine indicated proteins (each set of blots are representative of 3 independent experiments).

cell clumping. A 6-fold increase in the levels of EsxA was detected in the CF of *espK*::Tn cultured in Sauton's with tyloxapol compared to media without the detergent (Fig. 4B). Additionally, the level of EsxA in the CF of *espK*::Tn with tyloxapol was 2- to 3-fold more than that of WT *M. tuberculosis* grown without the detergent. Again, EspB (50 kDa) could not be detected in the CF of the *espK*::Tn strain regardless of whether or not tyloxapol was present (Fig. 4B). Approximately 8-fold more EsxA was detected in the CF of WT *M. tuberculosis* cultured with tyloxapol compared to culturing without detergent (Fig. 4B). On the other hand, EspB (50 kDa) levels in the CF of WT *M. tuberculosis* cultured with tyloxapol decreased by 60% relative to EspB levels in the CF of WT *M. tuberculosis* cultured without the detergent (Fig. 4B). Thus, the enhanced secretion of EsxA by *espK*::Tn is not due to Tween 80 alone.

In control experiments, the *espA*::Tn mutant, which does not secrete EsxA or EsxB (35), was also cultured for 3 days in Sauton's medium with or without detergents and analyzed. Interestingly, culturing the *espA*::Tn strain with Tween 80 but not tyloxapol resulted in the detection of a very small amount of EsxA in the CF (Fig. S2). Nevertheless, the level of EsxA released by the *espA*::Tn mutant in the presence of Tween 80 was much less than that of the *espK*::Tn mutant cultured in the presence of either Tween 80 or tyloxapol.

We also observed reductions ranging between 40% and 65% in the levels of Ag85 in the CFs of WT *M. tuberculosis*, *espA*::Tn, and *espK*::Tn strains when they were grown with detergents (Fig. 4A and B and Fig. S2). This and the reduced levels of EspB (50 kDa) in the CF of WT *M. tuberculosis* grown in the presence of detergents suggests the enhancement of EsxA levels in the CF are not due simply to detergent-mediated extraction or passive sloughing off of cell surface proteins.

These results collectively indicate that the delayed and reduced secretion of EsxA exhibited by EspK-deficient *M. tuberculosis* can be partially alleviated by detergents, but this does not appear to be the case for EspB secretion.

Trp-62 and Gly-64 in the conserved W-X-G motif of EspK is important for optimal EspB secretion. EspK contains a conserved W-X-G amino acid sequence motif of unknown functional importance, although it has been hypothesized to facilitate interaction with EspB (14) and with EspJ (11). This motif is also present in the ESX-1-secreted substrates EsxA, EsxB, and EspA and have been shown to be functionally important in these proteins (35). To examine whether Trp-62 (W62) and Gly-64 (G64) in the W-X-G

motif in EspK might be important for EsxA and EspB secretion, we cloned the *M. tuberculosis espK* gene alone along with its promoter into the shuttle vector pMD31 to obtain pMDespK^{WT}. Codons in *espK* encoding W62 and G64 in pMDespK^{WT} were replaced with codons encoding Arg (R) to generate pMDespK^{W62R} and pMDespK^{G64R}, respectively. These constructs as well as pMD31 (empty vector control) and pMDespK^{WT} were transformed into the *espK*::Tn mutant to obtain *espK*::Tn/pMD31, *espK*::Tn/pMDespK^{WT} (expressing WT EspK), *espK*::Tn/pMDespK^{W62R} (expressing EspK^{W62R}), and *espK*::Tn/pMDespK^{G64R} (expressing EspK^{G64R}) strains.

We and others have shown that the introduction of point mutations at conserved amino acid residues in different ESX-1-associated proteins can impact their expression or their stability (31, 35, 40). Therefore, we first assessed and compared cellular EspK levels in the CL fractions of WT *M. tuberculosis* and the transformed *espK*::Tn strains. With the exception of *espK*::Tn/pMD31, similar amounts of EspK proteins were detected in the CLs of WT *M. tuberculosis*, *espK*::Tn/pMDespK^{WT}, *espK*::Tn/pMDespK^{W62R}, and *espK*::Tn/pMDespK^{G64R} strains (Fig. 5A). Thus, replacement of the conserved W62 and G64 residues with Arg does not appear to affect the expression or stability of EspK.

We then analyzed the CF and CL fractions of WT *M. tuberculosis* and the complemented *espK*::Tn strains grown in Sauton's medium for 3, 5, and 7 days. Complementation with WT *espK* restored WT levels of EsxA and EspB secretion in the *espK*::Tn mutant (Fig. 5B). This confirms the transposon insertion does not cause any polar effects and likely impacts the *espK* gene alone. Strikingly, while EsxA secretion was fully restored to WT levels in the *espK*::Tn/pMDespK^{W62R} and *espK*::Tn/pMDespK^{G64R} strains, EspB secretion could only be partially restored in these two strains, with restoration being less in *espK*::Tn/pMDespK^{G64R} than *espK*::Tn/pMDespK^{W62R} (Fig. 5B). After 3 days of growth, no EspB (50 kDa) could be detected in the CFs of *espK*::Tn/pMDespK^{W62R} and *espK*::Tn/pMDespK^{G64R}, unlike in the CFs of WT *M. tuberculosis* and *espK*::Tn/pMDespK^{WT}. After 5 days, EspB (50 kDa) in the CFs of *espK*::Tn/pMDespK^{W62R} and *espK*::Tn/pMDespK^{G64R} had increased to 30 and 5%, respectively, of the EspB levels in the CFs of WT *M. tuberculosis* and *espK*::Tn/pMDespK^{WT}. By 7 days, EspB (50 kDa) in the CFs of *espK*::Tn/pMDespK^{W62R} and *espK*::Tn/pMDespK^{G64R} had reached 35 and 25%, respectively, of EspB levels in the CFs of WT *M. tuberculosis* and *espK*::Tn/pMDespK^{WT}. As expected, the control strain *espK*::Tn/pMD31 showed delayed EsxA secretion after 3 days of growth and complete lack of EspB secretion even after 7 days of growth (Fig. 5B).

These results clearly indicate the W-X-G motif in EspK is not important for the secretion of EsxA but is critical for optimal EspB secretion.

The conserved W-X-G motif of EspK is not important for its export or localization to the cell wall. Given that we found EspK is translocated to the cell wall of WT *M. tuberculosis*, we sought to determine the importance of the conserved W-X-G motif in this localization. Accordingly, CF, CW, CM, and cytosol fractions of *espK*::Tn/pMDespK^{WT}, *espK*::Tn/pMDespK^{W62R}, and *espK*::Tn/pMDespK^{G64R} strains were prepared and analyzed by immunoblotting. We detected equivalent amounts of EspK primarily in the CW fractions of the three strains (Fig. 6).

These results indicate the conserved W-X-G motif in EspK is not required for its export across the cytoplasmic membrane and localization to the cell wall.

Direct physical interaction between *M. tuberculosis* EspB and EspK requires the conserved W-X-G motif in EspK. Recombinant *M. tuberculosis* EspB and EspK have been shown to physically interact *in vitro* (24). To confirm this, an *Escherichia coli* strain coexpressing histidine-tagged full-length WT EspB and S-tagged WT EspK (*E. coli*/His tag EspB^{WT} + S tag EspK^{WT}) was generated and its lysate used in pulldown experiments. Control strains producing either histidine-tagged full-length WT EspB (*E. coli*/His tag EspB^{WT}) or S-tagged WT EspK (*E. coli*/S tag EspK^{WT}) proteins alone were also analyzed. We found cobalt magnetic Dynabeads captured histidine-tagged full-length EspB and in doing so also pulled down S-tagged EspK protein from *E. coli*/His tag EspB^{WT} + S tag EspK^{WT} lysates (Fig. 7A). In contrast, the same His tag Dynabeads did not capture S-tagged EspK protein from *E. coli*/S tag EspK^{WT} lysates (Fig. 7A). Conversely, the S-protein agarose beads captured S-tagged EspK and, in doing so, pulled down histidine-tagged
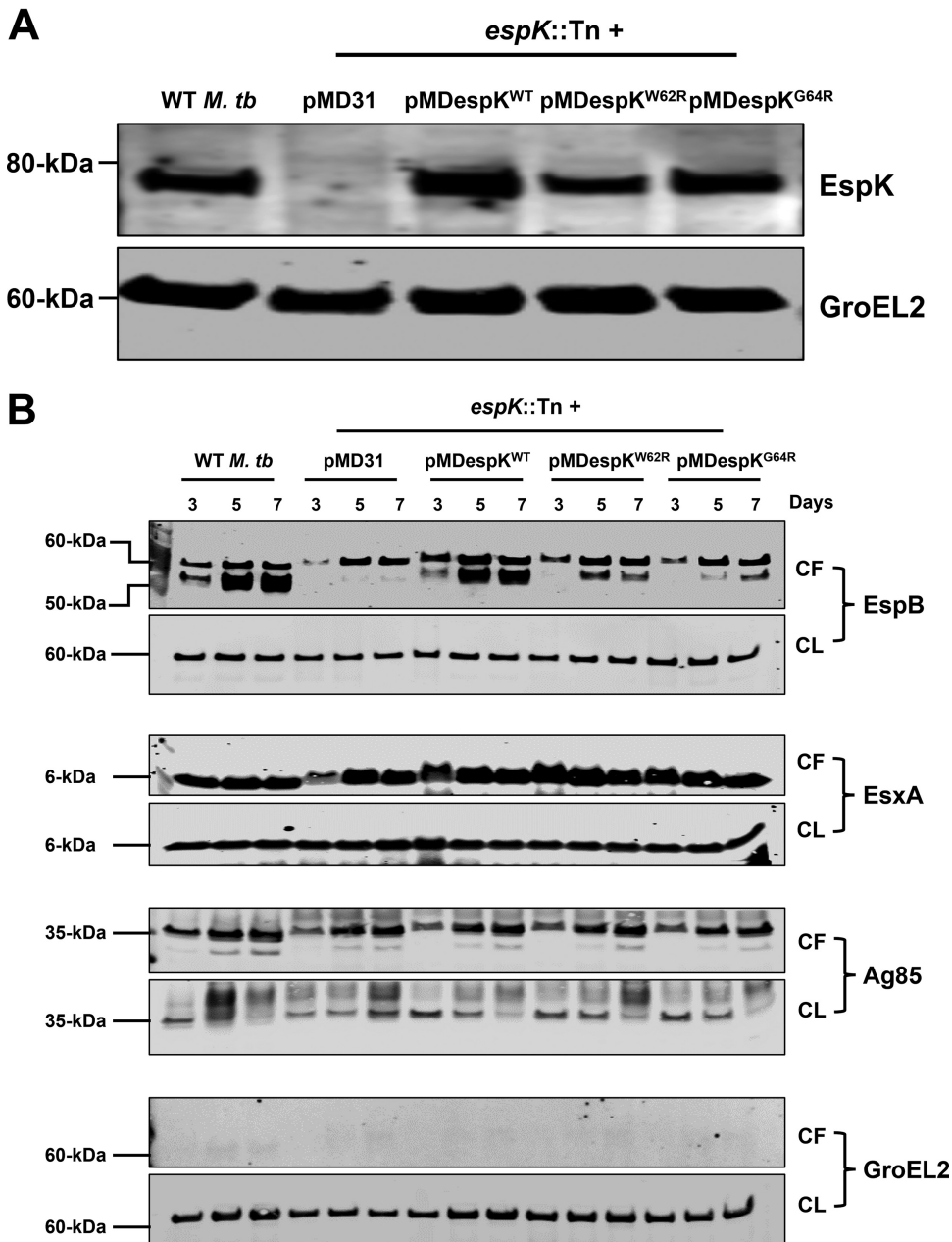
FIG 5 Secretion and expression of ESX-1 associated proteins by WT *M. tuberculosis* and complemented *espK*::Tn. (A and B) Immunoblots of CL proteins (5 μg/well) from WT *M. tuberculosis* and *espK*::Tn strain complemented with pMD31 (empty vector), pMDespK^WT, pMDespK^W62R, and pMDespK^G64R cultured 3 days in Sauton's medium without detergent to examine EspK levels (A) and CF (10 μg/well) and CL proteins (5 μg/well) from WT *M. tuberculosis* and *espK*::Tn strain complemented with pMD31, pMDespK^WT, pMDespK^W62R, and pMDespK^G64R cultured 3, 5, and 7 days in Sauton's medium without detergent (B) (each set of blots is representative of 3 independent experiments).

EspB from *E. coli*/His tag EspB^WT + S tag EspK^WT lysates (Fig. 7B). The same beads did not capture histidine-tagged EspB from *E. coli*/His tag EspB^WT lysates (Fig. 7B). These results are consistent with previous reports (24) that WT full-length EspB interacts with WT EspK.

We then examined if the conserved W62 and G64 residues in EspK are important for its interaction with EspB. Histidine-tagged full-length WT EspB with S-tagged EspK^WT, EspK^W62R, or EspK^G64R was coexpressed in *E. coli*, and the cell lysates were subjected to pulldown experiments. Compared to EspK^WT, significantly fewer EspK^W62R and EspK^G64R proteins were found to associate with histidine-tagged WT EspB captured by cobalt magnetic Dynabeads (Fig. 7C). In reciprocal pulldowns with S-protein agarose
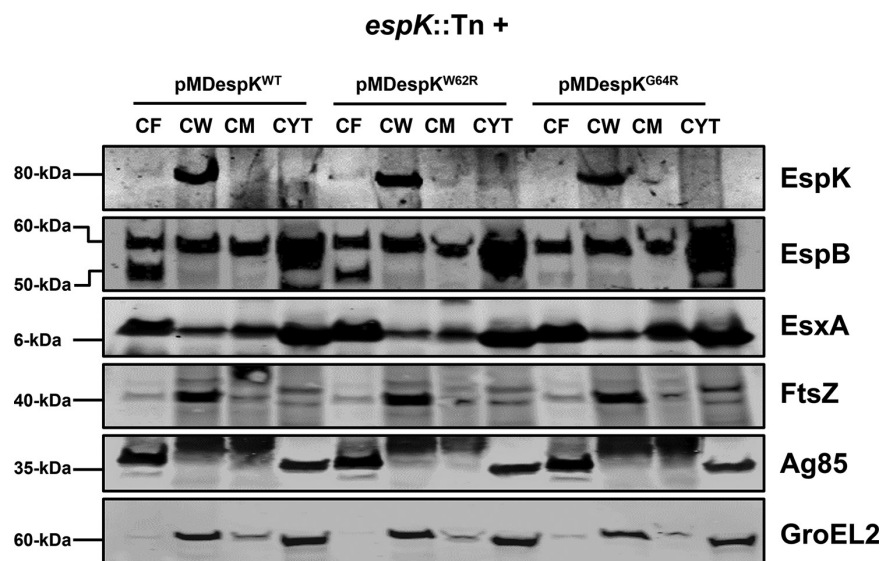
FIG 6 Importance of the conserved W-X-G motif to EspK export and cell wall localization. Immunoblots of 10 μg/well each of CF, CW, CM, and cytosol proteins from *espK*::Tn strain complemented with pMDespK^WT, pMDespK^W62R, and pMDespK^G64R (blot is representative of at least 2 independent experiments; L, protein ladder).

beads, noticeably less histidine-tagged WT EspB was found to associate with S-tagged EspK^W62R and EspK^G64R compared to S-tagged EspK^WT (Fig. 7D).

These results collectively indicate that the W-X-G motif in EspK is important for its interaction with EspB.

EspK prevents EspB from assembling into large macromolecular structures in the mycobacterial cell. Full-length EspB (60-kDa) found in *M. tuberculosis* CL has been shown by native PAGE to predominantly form low-order oligomers, while secreted EspB (50 kDa) in *M. tuberculosis* CF has been shown to form high-order oligomers (9). We hypothesized that EspK prevents EspB from prematurely adopting high-order macromolecular structures that are too large to pass through the cell membrane-spanning ESX-1 translocon complex. To test this notion, equivalent amounts of total CL proteins from WT *M. tuberculosis* and the *espK*::Tn strain were resolved by native PAGE and immunoblotted for EspB. Consistent with published data (9), we found the majority of EspB in the CL of WT *M. tuberculosis* formed low-order oligomers, with a small proportion assembling into high-order oligomers (denoted by the asterisk) (Fig. 8A). In contrast, a much higher proportion of EspB in the CL of *espK*::Tn seemed to assemble into high-order oligomers (Fig. 8A). This suggests that EspK is needed to maintain EspB at a lower oligomeric state inside the *M. tuberculosis* cell.

Since we have demonstrated that the conserved W-X-G motif of EspK is critical for its interaction with EspB and for EspB secretion, we reasoned the W62 and G64 residues in EspK are crucial in preventing EspB from forming high-order oligomers inside the *M. tuberculosis* cell. Indeed, native PAGE and immunoblotting revealed that full-length EspB in the CL of *espK*::Tn/pMDespK^WT formed predominantly low-order oligomers (Fig. 8B). In contrast, the CLs of *espK*::Tn/pMDespK^W62R, /pMDespK^G64R, and /pMD31 were found to contain progressively greater amounts of high-order EspB oligomers similar in size to the high-order EspB oligomers found in the CF of *espK*::Tn/pMDespK^WT (Fig. 8B). Strikingly, the presence of greater amounts of high-order EspB oligomers in the CL of *espK*::Tn/pMDespK^G64R compared to what is found in the CL of *espK*::Tn/pMDespK^W62R correlates well with the poorer restoration of EspB secretion exhibited by *espK*::Tn/pMDespK^G64R compared to *espK*::Tn/pMDespK^W62R (Fig. 8B).

Collectively, these results strongly suggest that the interaction of EspK with EspB is required by *M. tuberculosis* to maintain cytosolic EspB as lower-order oligomers and that the conserved W-X-G motif in EspK is critical for this function.
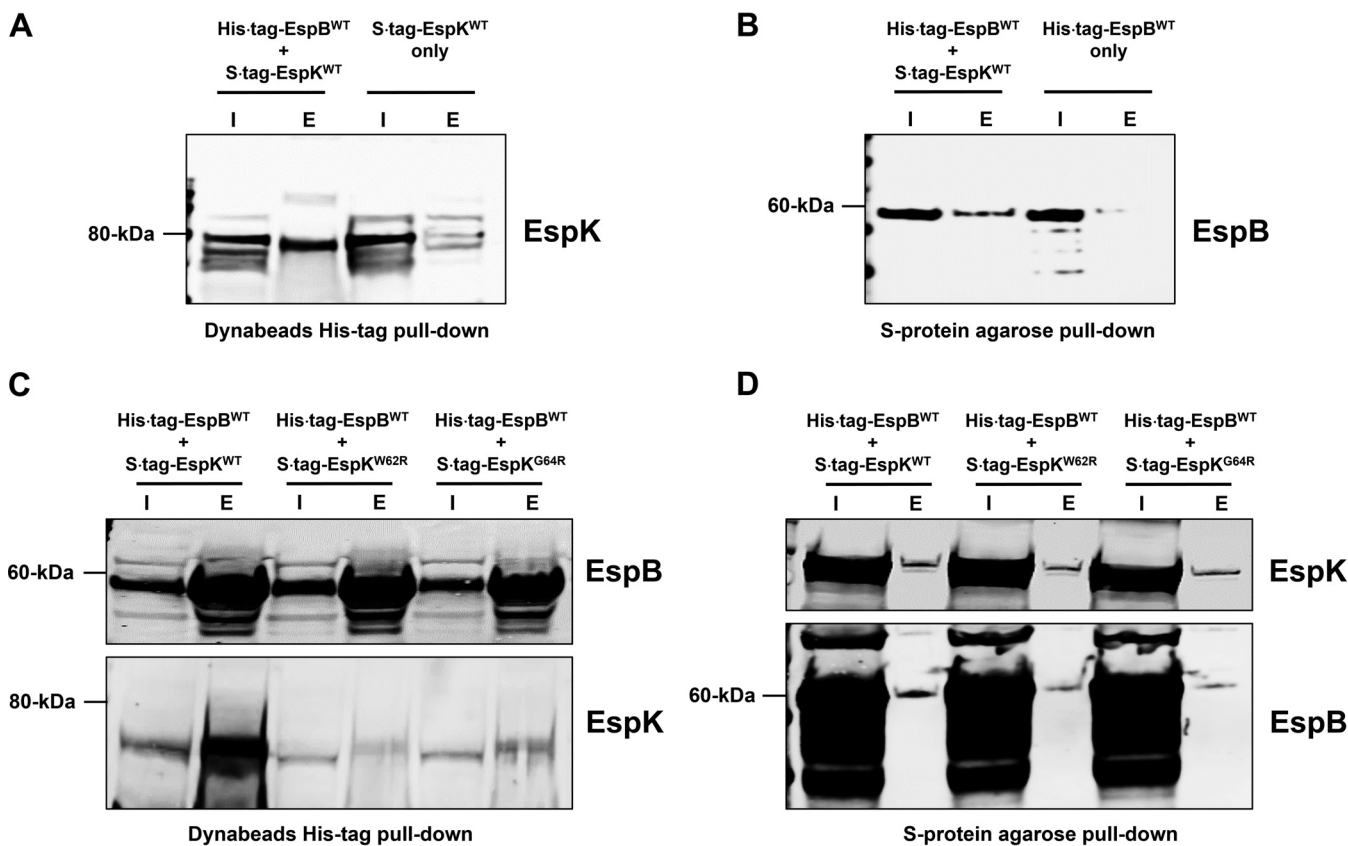
FIG 7 Pulldown analysis of EspB and EspK coexpressed in *E. coli*. (A and B) Immunoblots of EspK pulled down by His tag Dynabeads from the lysates of *E. coli*/His tag EspB^{WT} + S tag EspK^{WT} and *E. coli*/S tag EspK^{WT} (A) and EspB pulled down by S-protein agarose beads from the lysates of *E. coli*/His tag EspB^{WT} + S tag EspK^{WT} and *E. coli*/His tag EspB^{WT} (B). (C and D) Immunoblots of EspB and EspK pulled down by His tag Dynabeads (C) and S-protein agarose beads (D) from the lysates of *E. coli*/His tag EspB^{WT} + S tag EspK^{WT}, *E. coli*/His tag EspB^{WT} + S tag EspK^{W62R}, and *E. coli*/His tag EspB^{WT} + S tag EspK^{G64R} (each set of blots is representative of at least 2 independent experiments; I, input 5 μg of lysates; E, all proteins eluted from beads in 50 μL of SDS-PAGE sample buffer).

DISCUSSION

In this study, we sought to understand the function of EspK in *M. tuberculosis* and found this W-X-G motif-containing protein plays an active, multifaceted role in the type-7 secretion system ESX-1 of the tubercle bacillus.

The unique ESX-1 secretion defects of the *M. tuberculosis espK*::Tn strain described here are consistent with what is seen in EspK-deficient *M. marinum* (22, 24). However, one salient feature of *M. tuberculosis* EspK that we have uncovered in our study is that it facilitates EsxA and EspB secretion in *M. tuberculosis* through distinct pathways, and we have multiple lines of evidence to support this contention. First, we show that EsxA secretion by EspK-deficient *M. tuberculosis* is delayed and reduced rather than being completely blocked, as is the case with EspB. Second, by culturing EspK-deficient *M. tuberculosis* in detergent-containing media, we were able to restore secretion of EsxA, but not EspB, to WT *M. tuberculosis* levels. The detergent-dependent enhancement of EsxA secretion by *espK*::Tn and WT *M. tuberculosis* strains observed here appears to be consistent with the observations of Raffetseder et al. in that culturing WT *M. tuberculosis* with Tween 80 results in the release of EsxA from the mycobacterial cell surface (41). However, the reduced secretion of Ag85 by WT *M. tuberculosis*, *espA*::Tn, and *espK*::Tn strains and the reduced secretion of EspB by WT *M. tuberculosis* when cultured in detergent-containing media suggest the enhancement of EsxA secretion is not simply due to the passive sloughing off of cell surface-localized proteins but rather through an indeterminate mechanism. Third, through complementation experiments, we show that optimal EsxA secretion can be restored by episomal expression of the WT *espK* gene as well as by alleles bearing W62R and G64R mutations. In contrast, EspB
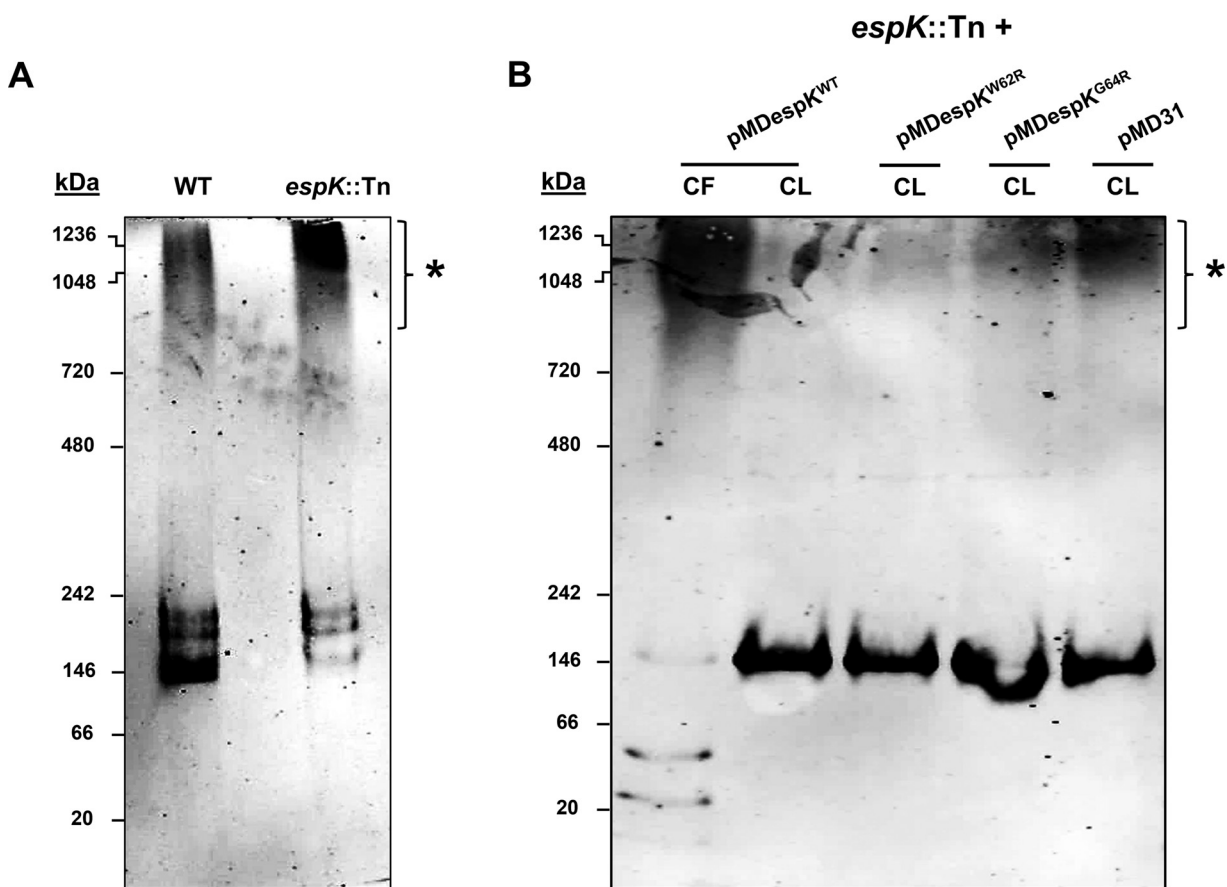
FIG 8 EspB native conformation analysis. (A and B) Native PAGE and EspB immunoblots of CL proteins (5 μg/well) from wild-type *M. tuberculosis* Erdman (WT) and *espK*::Tn strain cultured for 3 days in Sauton's medium without Tween 80 (A) and CF protein (10 μg/well) of *espK*::Tn complemented with pMDespK^{WT} and CL proteins (5 μg/well) of *espK*::Tn complemented with pMDespK^{WT}, pMDespK^{W62R}, pMDespK^{G64R}, and pMD31 cultured for 4 days in Sauton's medium without detergent (B) (each set of blots are representative of at least 2 independent experiments; asterisks indicate higher-order oligomers of EspB).

secretion is disrupted by the same mutations in the W-X-G motif of EspK. Further indirect support comes from observations of *M. leprae* where *espB*, *espJ*, *espK*, and *pe35* are all pseudogenes (42), and despite this, its residual streamlined ESX-1 apparatus still secretes EsxA and EsxB to exert virulence effects during infection (26, 29).

Another salient feature of *M. tuberculosis* EspK uncovered here is that it is exported and localized by the tubercle bacillus to its cell wall and not to the extracellular milieu. Given that the production of EsxA and EsxB proteins in the *M. tuberculosis* cell are vital to ESX-1 secretion activity, the unimpeded translocation of EspK across the cytoplasmic membrane to the cell wall in the EsxA- and EsxB-deficient 5′Tn::*pe35* strain indicates EspK export in *M. tuberculosis* is ESX-1 independent. This is different from what has been reported in *M. marinum*, where its EspK is secreted in an ESX-1-dependent manner to the capsule and beyond (20–22). We also have reason to believe *M. tuberculosis* EspK is not localized to its capsule, because during the process of subcellular fractionation, the *M. tuberculosis* cells were subjected to vigorous shaking with silica beads to lyse cells. This action is known to disrupt the mycobacterial capsule and would have released all of its constituents into the lysis buffer solution (43). If EspK were exported by the tubercle bacillus to its capsule like *M. marinum*, the protein would have ended up in the cytosolic fraction after multiple rounds of ultracentrifugation. This was not observed, and most of the EspK was found associated with the cell wall fraction instead. Clearly, despite the similarities in *M. tuberculosis* and *M. marinum* ESX-1 systems, our observations highlight evolutionary differences that likely reflect the human-

specific virulence adaptations of *M. tuberculosis* and generalized virulence as well as free-living aquatic adaptations of *M. marinum* (1, 44). Along these lines, it is also notable that *M. marinum* possesses two orthologs of EspK, encoded by MMAR_5455 and MMAR_4351 (18, 19). While the EspK ortholog encoded by MMAR_5455 is associated with *M. marinum* ESX-1, the function of the other, encoded by MMAR_4351, remains a mystery (18, 19). It is also notable that both orthologs share very similar amino acid sequence identities with *M. tuberculosis* EspK. Clustal alignments show MMAR_5455 encoding *M. marinum* EspK shares approximately 56% amino acid sequence identity with *M. tuberculosis* EspK (see Fig. S5A in the supplemental material), while the protein encoded by MMAR_4351 shares approximately 54% amino acid sequence identity with *M. tuberculosis* EspK (Fig. S5B) (45). Another example that highlights differences between the *M. tuberculosis* and *M. marinum* ESX-1 systems is that of $EspG_1$ encoded by a gene in the extended RD1 region of the *esx-1* locus. While $EspG_1$ is required for EsxA and EsxB secretion and virulence in *M. marinum* (23), the homolog of this protein in *M. tuberculosis* is dispensable for ESX-1-mediated secretion and immunogenicity but not for virulence (46). Finally, that EspK is released into the extracellular milieu by *M. marinum* but not by *M. tuberculosis* is also consistent with the existence of a more extensive repertoire of ESX-1 secreted protein substrates in *M. marinum* (22, 44).

Our demonstration that the conserved W-X-G motif in EspK is critical for EspB secretion for its interaction with EspB and maintenance of EspB inside the *M. tuberculosis* cell at low-order oligomeric states is another notable outcome of this study. An explanation for how EspK might facilitate the secretion of EspB may be found in the structure of the EspB protein itself. Unusually, this ESX-1 protein, which seems to have arisen from a gene fusion, contains both the W-X-G and Y-X-X-X-D secretion motifs (9–11). Crystal structures and the cryoelectron microscopy (cryo-EM) map of pure EspB reveal a hydrogen bond between the nitrogen atom of the tryptophan in the W-X-G motif and the oxygen atom of tyrosine in the Y-X-X-X-D motif of adjacent monomers in this ring-shaped heptameric protein (9–11). However, while EspB is inside the *M. tuberculosis* cell, it has been shown to adopt predominantly dimeric and tetrameric states, but after translocation, secreted EspB assumes a conformation consisting of high-order oligomers consistent with ring-shaped heptameric structures (9). While it has been proposed that the protein pairs EspA-EspC, EspE-EspF, and EspJ-EspK are cosecreted (11), we have shown here and previously (7) that EspB is not cosecreted with other known ESX-1 substrates by *M. tuberculosis*. We propose that interaction between the conserved W-X-G motif of EspK and the Y-X-X-X-D motif of EspB inside the *M. tuberculosis* cell somehow maintains the latter in a lower oligomeric state until EspK interacts with $EccCa_1$–$EccCb_1$, a membrane-associated ATPase component of the membrane-localized ESX-1 translocon complex that presumably powers the translocation of EspB (24). After exiting the cell, EspB could then oligomerize via interactions between its own W-X-G and Y-X-X-X-D motifs on adjacent monomers to form the heptameric ring-like structure. In the absence of EspK, premature high-order oligomeric assembly of EspB inside the *M. tuberculosis* cell could result in a macromolecule that is either unable to engage with or too large to pass through the ESX-1 translocon complex. Indeed, this notion is supported by our finding that in *M. tuberculosis* either deficient in EspK or expressing $EspK^{W62R}$ and $EspK^{G64R}$, EspB exists as high-order oligomers in greater proportions. Whether EspK prevents EspB from forming high-order homo-oligomers and/or high-order hetero-oligomers with other *M. tuberculosis* proteins is currently not known and requires further study. It is also not known if EspK interacts with newly synthesized and unfolded EspB to prevent oligomerization or if EspK actively uncouples high-order oligomers of EspB. The latter is unlikely, as this would require energy from ATP hydrolysis and no ATPase domains have been detected in EspK. Finally, it is not known if the ESX-1-independent movement of EspK across the *M. tuberculosis* cytoplasmic membrane has any impact on its ability to maintain cytosolic EspB at low-order oligomeric states and enable its secretion through the ESX-1 translocon core. The generation and characterization of *M. tuberculosis* mutants that are unable to export EspK will help clarify this question.

Our observation that EspK-deficient *M. tuberculosis* strains are not compromised in their ability to induce macrophage cell death or replicate in mice is consistent with what is seen in EspK-deficient *M. bovis* (12, 15) and also *M. africanum* to some extent (16). The apparent lack of virulence defects in the *M. tuberculosis espK*::Tn strain is, however, not consistent with what is seen in EspK-deficient *M. marinum* (22–25) and likely reflects differences between these two separate species of mycobacteria. Despite the secretion defects observed *in vitro*, we cannot rule out the possibility that the *espK*::Tn strain can still secrete sufficient amounts of EsxA to kill macrophages and replicate in the lungs and spleens of mice. Indeed, we have previously isolated *M. tuberculosis* mutants expressing variants of EspA that exhibit ESX-1 secretion defects *in vitro* but undiminished cytopathy toward macrophages and replication in mice compared to WT *M. tuberculosis* (35). Moreover, culturing the *espK*::Tn strain in detergent-containing media and restoration of WT levels of EsxA secretion may also prevent reductions in its virulence. Still, understanding why the *espK*::Tn strain remains virulent is crucial in light of our previous finding that secreted EspB possesses a virulence function that is distinct from that of EsxA and EsxB (7). One possibility is that the continued secretion of EsxA (and presumably its cosecreted partner proteins) by the *espK*::Tn strain obscures the attenuation of virulence resulting from the lack of EspB secretion alone. Indeed, we were only able to detect EspB-mediated macrophage cell death and replication in mice through direct comparisons of the EsxA and EsxB secretion-defective but EspB secretion-competent *M. tuberculosis espA*::Tn strain and the isogenic 5′Tn::*pe35* strain that is unable to secrete EsxA, EsxB, or EspB (7). It is also possible that secreted EspB mediates aspects of *M. tuberculosis* virulence that the macrophage cell death assay and *in vivo* replication study performed here simply cannot detect. For instance, the resazurin-based PrestoBlue reagent was used here to measure respiration of viable macrophages and quantify THP-1 macrophage survival after infection with *M. tuberculosis* (7, 32, 35). However, this readout does not provide information on the type of cell death induced. This is important, because while some modes of programmed cell death enhance TB pathogenesis, others are host-protective and actively subverted by *M. tuberculosis* (47, 48). As such, it is possible WT *M. tuberculosis* induces macrophage cell death that is detrimental to the host while *espK*::Tn induces macrophage cell death of the same magnitude that might benefit a host. Even though the *espK*::Tn strain replicates as well as WT *M. tuberculosis* in mice, it remains to be determined if animals infected with EspK-deficient *M. tuberculosis* exhibit decreased pathology and/or increased survival compared to those infected with WT *M. tuberculosis*. Indeed, an *M. tuberculosis* mutant expressing a serine protease dead variant of $MycP_1$ was found to replicate as well as WT *M. tuberculosis* in macrophages and in the lungs of mice but was not as lethal as its WT counterpart (6). Finally, it has been shown that *M. africanum* and *M. marinum* EspK-deficient mutants poorly induce beta interferon (IFN-β) production in macrophages (25, 49, 50). This is noteworthy because type I IFN responses are critical for TB pathogenesis (51, 52). It is also noteworthy that *M. africanum* reportedly induces less pathology in mice (17). Might some of these unique virulence features of *M. africanum* be due to its lack of EspK and inability to secrete EspB? Indeed, in unpublished work we have found that *M. africanum* is unable to secrete EspB despite being able to secrete EsxA (Fig. S6).

In conclusion, the characterization of an EspK-deficient *M. tuberculosis* mutant strain in this study has provided new insights into the function of an ESX-1 component. Our confirmation that *M. tuberculosis* EspK is an active and crucial participant in the ESX-1 system demonstrates once again the complexity of this unique secretion machine.

MATERIALS AND METHODS

Enzymes and reagents. DNA-modifying enzymes and high-fidelity Phusion DNA polymerase were purchased from New England Biolabs (Ipswich, MA, USA). Oligonucleotides were purchased from Integrated DNA Technologies (Coralville, IA, USA). All other chemicals and reagents used were purchased from Sigma-Aldrich (Oakville, ON, Canada).

Bacterial strains and growth conditions. Except where indicated, *M. tuberculosis* strains were routinely cultured in Middlebrook 7H9 liquid medium (Becton, Dickinson) supplemented with 0.2% glycerol,

10% albumin-dextrose-catalase (ADC), and 0.05% detergent Tween 80 or on 7H11 agar (Becton, Dickinson) supplemented with 0.5% glycerol, 10% oleic acid-albumin-dextrose-catalase (OADC). Generation of *M. tuberculosis* Erdman Tn*5370* transposon insertion mutants (*espA*::Tn and *espK*::Tn) has been described previously (30). Transposon insertion mutants were cultured in the presence of hygromycin.

Cloning and plasmid vector construction. Construction of plasmid vectors used in this study was as follows.

(i) pMDespK and derivatives. *espK* with its native promoter was amplified by PCR from the 2F9 cosmid using the primer pair 5′-CGC**TCTAGA**TGGCGTGAGTACGCATTGTC-3′ and 5′-CGC**TCTAGA**GTCCACG AAGTGACAAACGA-3′ (XbaI site in boldface). The *espK* fragment was cloned into pMD31 to yield pMDespK^{WT} and verified by DNA sequencing. Site-specific mutagenesis of pMDespK^{WT} using the QuikChange mutagenesis system (Agilent Technologies) to replace EspK amino acid residues Trp-62 (W62) and Gly-64 (G64) with Arg was done using mutagenic oligonucleotide pairs 5′-GAAGGCGGCCTACGGTCCGGCGGCGCC-3′ and 5′-GGCG CCGCCGGACCGTAGGCCGCCTTC-3′ as well as 5′-GGCCTATGGTCCCGCGGCGCCGCCAAT-3′ and 5′-ATTGGCGG CGCCGCGGGACCATAGGCC-3′, respectively. Mutagenized constructs were verified by DNA sequencing. pMD31, pMDespK^{WT}, pMDespK^{W62R}, and pMDespK^{G64R} were electroporated into the *espK*::Tn mutant strain and selected on kanamycin. *espK*::Tn/pMD31, *espK*::Tn/pMDespK^{WT} (expressing WT EspK), *espK*::Tn/pMDespK^{W62R} (expressing EspK^{W62R}), and *espK*::Tn/pMDespK^{G64R} (expressing EspK^{G64R}) strains were generated accordingly.

(ii) pETDuet-espB+espK and derivatives. Full-length *espB* encoding the 60-kDa EspB cytosolic iso-form was amplified by PCR from 2F9 using the primer pair 5′-CAG**GAATTC**TATGACGCAGTCGCAGA CCGTGACG-3′ and 5′-CGC**AAGCTT**TCACTTCGACTCCTTACTGTCCTGG-3′ (EcoRI and HindIII sites in bold-face) and cloned into the pETDuet vector (Sigma-Aldrich) to obtain pETDuet-espB encoding N terminus histidine-tagged full-length EspB. *espK* was amplified by PCR from pMDespK^{WT}, pMDespK^{W62R}, and pMDespK^{G64R} using the primer pair 5′-CAAGCC**AGATCT**ATGAGTATTACCAGGCCGACGG-3′ and 5′-CA AGCC**GCGATCGC**TCAGCATGCGGCGGCCAG-3′ (BglII and AsiSI sites in boldface) and subcloned into pETDuet-espB to obtain pETDuet-espB+espK^{WT}, pETDuet-espB+espK^{W62R}, and pETDuet-espB+espK^{G64R}, respectively. These encode C-terminal S-tagged EspK proteins (53). All constructs were verified by DNA sequencing. pETDuet-espB+espK^{WT}, pETDuet-espB+espK^{W62R}, and pETDuet-espB+espK^{G64R} were trans-formed into *Escherichia coli* strain LOBSTR-BL21-DE3 (Kerafast) and selected on ampicillin to provide *E. coli*/His tag EspB^{WT} + S tag EspK^{WT}, *E. coli*/His tag EspB^{WT} + S tag EspK^{W62R}, and *E. coli*/His tag EspB^{WT} + S tag EspK^{G64R} strains, respectively. Control *E. coli* strains transformed with pETDuet-espB and pETDuet-espK^{WT} and producing histidine-tagged full-length WT EspB (*E. coli*/His tag EspB^{WT}) and S-tagged WT EspK (*E. coli*/S tag EspK^{WT}), respectively, were also generated for use as controls.

***M. tuberculosis* culture conditions and protein preparation for immunoblots.** *M. tuberculosis* strains were cultured for immunoblot analysis as described previously (7, 31, 35, 54). Briefly, colonies picked from 7H11 agar plates were cultured first in 7H9 broth to an optical density at 600 nm (OD$_{600}$) of ~1.5 and subcultured into Sauton's medium supplemented with 0.05% Tween 80 at a starting OD$_{600}$ of 0.1. Cells were grown to mid-log phase (OD$_{600}$ of 0.6 to 0.8) and then centrifuged. The cell pellet was washed once with phosphate-buffered saline (PBS) before resuspending in Sauton's medium without detergent (unless otherwise indicated) with a starting OD$_{600}$ of 0.2 to 0.5 and cultured further for the indicated number of days at 37°C with agitation. Cell cultures were centrifuged to separate supernatant and bacteria. Supernatants were filtered through 0.4- and 0.2-μm filters to remove bacterial cells prior to removal from biocontainment. Culture filtrate (CF) proteins were concentrated in Vivaspin columns (Sartorius) with 5-kDa-molecular-weight-cutoff membranes. Cell lysate (CL) proteins were prepared by resuspending cell pellets in lysis buffer (PBS containing Roche protease inhibitor cocktail tablets) and bead beating using 100-μm zirconia beads and clarified by centrifugation. Total protein concentrations were determined using the bicinchoninic acid (BCA) assay (ThermoFisher) with bovine serum albumin (BSA) as the standard.

Subcellular fractionation of *M. tuberculosis* cells. The cell wall (which includes the mycomem-brane or outer membrane and peptidoglycan layer), cytoplasmic membrane, and cytosol protein frac-tions of *M. tuberculosis* were prepared using well-established methods described previously (36–38). Briefly, CL obtained after bead beating of *M. tuberculosis* cell pellets with zirconia beads were ultracentri-fuged at 27,000 × *g* for 1 h at 4°C. The resulting pellets were suspended in lysis buffer and vortexed to yield cell wall protein fractions. The supernatants from this step were ultracentrifuged further at 100,000 × *g* for 4 h at 4°C. The resulting pellets were suspended in lysis buffer and vortexed to yield cytoplasmic membrane protein fractions. The supernatants from this ultracentrifugation step yielded the cytosolic protein fractions. Total protein concentrations of these fractions were determined using the BCA assay with bovine serum albumin as the standard.

Immunoblotting. Immunoblotting was done as described previously (7, 31, 35, 54). Briefly, indicated amounts of CF or CL proteins were separated in NuPAGE 4 to 12% Bis-Tris gels (ThermoFisher) and trans-ferred to nitrocellulose membranes using the iBlot system (ThermoFisher). Membranes were then blocked with TBS-milk (20 mM Tris-HCl, pH 7.5, 150 mM NaCl, and 5% nonfat milk powder) and incu-bated overnight with the desired primary antibody diluted in TNT-BSA (20 mM Tris-HCl, pH 7.5, 150 mM NaCl, 0.05% Tween 20 and 1% BSA fraction V) at 4°C. Membranes were washed with TNT (20 mM Tris-HCl, pH 7.5, 150 mM NaCl, 0.05% Tween 20), incubated with the appropriate fluorescent secondary anti-body in TNT-BSA, washed three times with TNT, and scanned using the Odyssey CLx imaging system (LI-COR Biosciences). GroEL2 was used as a lysis control for culture filtrates and as a loading control for cell lysates. ESX-1-independent secreted protein Ag85 was probed as a loading control for culture filtrates. Polyclonal rabbit antibodies against EspK (Statens Serum Institute; a gift from Ida Rosenkrands) were used at a dilution of 1:400. Polyclonal rat antibodies against recombinant full-length EspB were generated for us by Kaneka Eurogentec S.A. and verified to specifically detect EspB (Fig. S3). These rat anti-EspB antibodies

were used at a dilution of 1:1,000. Mouse monoclonal antibodies against EsxA, EsxB, and GroEL2 and rabbit polyclonals against Ag85 were used at dilutions of 1:4,000.

Recombinant histidine-tagged EspB and S-tagged EspK coexpression in *E. coli* and pulldown assays. *E. coli*/His tag EspB^{WT} + S tag EspK^{WT}, *E. coli*/His tag EspB^{WT} + S tag EspK^{W62R}, and *E. coli*/His tag EspB^{WT} + S tag EspK^{G64R} were cultured in 10 mL LB medium (plus 100 μg/mL ampicillin) at 37°C overnight and then subcultured in 200 mL of the same medium. His tag EspB and S tag EspK coexpression was induced at 16°C overnight with 1 mM IPTG. *E. coli* cell pellets were resuspended in lysis buffer (50 mM NaH$_2$PO$_4$, 300 mM NaCl, pH 8, EDTA-free protease inhibitor) and lysed in an Emulsiflex C3 homogenizer (Avestin). Lysates were clarified by centrifugation at 10,000 $\times$ *g* for 30 min at 4°C and protein concentrations determined by BCA assay. Clarified lysates were used in pulldown assays.

To pull down EspK with immobilized His tag EspB, cobalt-based magnetic His tag beads (Dynabeads-ThermoFisher) were used. Briefly, 500 μg of *E. coli* cell lysate protein in 750 μL of binding/wash buffer (50 mM NaH$_2$PO$_4$, 300 mM NaCl, pH 8, plus 0.01% Tween 20) was incubated with 200 μl of beads overnight at 4°C with gentle mixing. Magnetically immobilized beads were then washed 5 times with 500 μl of binding/wash buffer before boiling beads in 50 μL of 1$\times$ SDS-PAGE sample loading buffer at 95°C for 10 min. The eluted proteins (E) from the boiled beads in this 50 μL were all loaded along with 5 μg of input lysate (I) in NuPAGE 4 to 12% Bis-Tris gels (ThermoFisher), separated, and immunoblotted as described above. NuPAGE gels of the same were also Coomassie stained to verify the total amounts of proteins in input lysates from different strains were equivalent and that the pulled down and eluted proteins from different strains were also equivalent (Fig. S4).

In reciprocal pulldown experiments to capture EspB through immobilization of S tag EspK, S-protein agarose beads (Millipore) were used (53). In this case, 1 mg of *E. coli* cell lysate protein in 500 μL of binding/wash buffer (50 mM NaH$_2$PO$_4$, 300 mM NaCl, pH 8, plus 0.01% Tween 20) was incubated with 120 μl of beads overnight at 4°C with gentle mixing. Beads were washed after gentle centrifugation 3 times with 500 μl of binding/wash buffer. Captured proteins were eluted by boiling beads in 50 μL of 1$\times$ SDS-PAGE loading buffer at 95°C for 10 min. Eluted proteins (E) from the boiled beads in this 50 μL were all loaded along with 20 μg of input lysate (I) in NuPAGE 4 to 12% Bis-Tris gels, separated, and immunoblotted as described above.

Rat polyclonal against EspB at 1:1,000 dilution and rabbit polyclonal EspK antibody at 1:400 dilution were used to detect EspB and EspK, respectively.

Native PAGE of cell lysate proteins. Native PAGE and immunoblotting were done as described previously (9). Briefly, indicated amounts of proteins were resolved in Novex 4 to 12% Tris-glycine gels (ThermoFisher), transferred to nitrocellulose membranes using the iBlot system (ThermoFisher), and processed as described above.

THP-1 cell death assays. *M. tuberculosis* strains for THP-1 human macrophage infections were cultured axenically in 7H9 with ADC and 0.05% Tween 80. After measuring the OD$_{600}$ and calculating the number of CFU per milliliter, aliquots of the bacteria were added to RPMI medium (supplemented with 10% fetal bovine serum) to obtain the required OD$_{600}$ and used to infect THP-1 cells at a multiplicity of infection (MOI) of 5. Survival of THP-1 cells 3 days postinfection was determined using the PrestoBlue reagent (ThermoFisher) as described previously (7, 35, 54, 55).

Mouse infection. *M. tuberculosis* strains for mouse infections were axenically cultured in 7H9 with ADC and 0.05% Tween 80. After measuring the OD$_{600}$ and calculating the number of CFU per milliliter, aliquots of the bacteria were added to PBS at the required number of CFU per milliliter for aerosol infections. Mice were challenged with $\sim$200 CFU of either WT *M. tuberculosis* or *espK*::Tn mutant via the aerosol route using a custom-built aerosol exposure unit (Madison Exposure Chambers, LLC). Animal use protocols were reviewed and approved by the chief veterinarian of the Swiss Federal Institute of Technology, by the Service de la Consommation et des Affaires Vétérinaires of the Canton of Vaud, and by the Swiss Office Vétérinaire Fédéral. Lung and spleen bacterial burden in CFU were enumerated at 3 and 6 weeks postinfection.

Statistical analysis. ImageJ was used to perform densitometric analysis of immunoblots. GraphPad Prism was used to determine statistical differences in cell death induced in THP-1 cells infected with *M. tuberculosis* strains and replication of *M. tuberculosis* strains in lungs and spleens of mice.

SUPPLEMENTAL MATERIAL

Supplemental material is available online only.

SUPPLEMENTAL FILE 1, PDF file, 0.7 MB.

(NR-44103), GroEL2 (NR-13825), Antigen-85 complex (NR-13800), and *M. tuberculosis* H37Rv subcellular fractions were obtained through BEI Resources, NIAID, NIH.

REFERENCES

1. Bottai D, Groschel MI, Brosch R. 2017. Type VII secretion systems in Gram-positive bacteria. Curr Top Microbiol Immunol 404:235–265. https://doi.org/10.1007/82_2015_5015.

2. Beckham KS, Ciccarelli L, Bunduc CM, Mertens HD, Ummels R, Lugmayr W, Mayr J, Rettel M, Savitski MM, Svergun DI, Bitter W, Wilmanns M, Marlovits TC, Parret AH, Houben EN. 2017. Structure of the mycobacterial ESX-5 type VII secretion system membrane complex by single-particle analysis. Nat Microbiol 2:17047. https://doi.org/10.1038/nmicrobiol.2017.47.

3. Famelis N, Rivera-Calzada A, Degliesposti G, Wingender M, Mietrach N, Skehel JM, Fernandez-Leiro R, Bottcher B, Schlosser A, Llorca O, Geibel S. 2019. Architecture of the mycobacterial type VII secretion system. Nature 576:321–325. https://doi.org/10.1038/s41586-019-1633-1.

4. Groschel MI, Sayes F, Simeone R, Majlessi L, Brosch R. 2016. ESX secretion systems: mycobacterial evolution to counter host immunity. Nat Rev Microbiol 14:677–691. https://doi.org/10.1038/nrmicro.2016.131.

5. Poweleit N, Czudnochowski N, Nakagawa R, Trinidad DD, Murphy KC, Sassetti CM, Rosenberg OS. 2019. The structure of the endogenous ESX-3 secretion system. Elife 8:e52983. https://doi.org/10.7554/eLife.52983.

6. Ohol YM, Goetz DH, Chan K, Shiloh MU, Craik CS, Cox JS. 2010. Mycobacterium tuberculosis MycP1 protease plays a dual role in regulation of ESX-1 secretion and virulence. Cell Host Microbe 7:210–220. https://doi.org/10.1016/j.chom.2010.02.006.

7. Chen JM, Zhang M, Rybniker J, Boy-Rottger S, Dhar N, Pojer F, Cole ST. 2013. Mycobacterium tuberculosis EspB binds phospholipids and mediates EsxA-independent virulence. Mol Microbiol 89:1154–1166. https://doi.org/10.1111/mmi.12336.

8. Gijsbers A, Vinciauskaite V, Siroy A, Gao Y, Tria G, Mathew A, Sanchez-Puig N, Lopez-Iglesias C, Peters PJ, Ravelli RBG. 2021. Priming mycobacterial ESX-secreted protein B to form a channel-like structure. Curr Res Struct Biol 3:153–164. https://doi.org/10.1016/j.crstbi.2021.06.001.

9. Korotkova N, Piton J, Wagner JM, Boy-Rottger S, Japaridze A, Evans TJ, Cole ST, Pojer F, Korotkov KV. 2015. Structure of EspB, a secreted substrate of the ESX-1 secretion system of Mycobacterium tuberculosis. J Struct Biol 191:236–244. https://doi.org/10.1016/j.jsb.2015.06.003.

10. Piton J, Pojer F, Wakatsuki S, Gati C, Cole ST. 2020. High resolution CryoEM structure of the ring-shaped virulence factor EspB from Mycobacterium tuberculosis. J Struct Biol X 4:100029. https://doi.org/10.1016/j.yjsbx.2020.100029.

11. Solomonson M, Setiaputra D, Makepeace KAT, Lameignere E, Petrotchenko EV, Conrady DG, Bergeron JR, Vuckovic M, DiMaio F, Borchers CH, Yip CK, Strynadka NCJ. 2015. Structure of EspB from the ESX-1 type VII secretion system and insights into its export mechanism. Structure 23:571–583. https://doi.org/10.1016/j.str.2015.01.002.

12. Brodin P, Majlessi L, Marsollier L, de Jonge MI, Bottai D, Demangel C, Hinds J, Neyrolles O, Butcher PD, Leclerc C, Cole ST, Brosch R. 2006. Dissection of ESAT-6 system 1 of Mycobacterium tuberculosis and impact on immunogenicity and virulence. Infect Immun 74:88–98. https://doi.org/10.1128/IAI.74.1.88-98.2006.

13. Cole ST, Eiglmeier K, Parkhill J, James KD, Thomson NR, Wheeler PR, Honore N, Garnier T, Churcher C, Harris D, Mungall K, Basham D, Brown D, Chillingworth T, Connor R, Davies RM, Devlin K, Duthoy S, Feltwell T, Fraser A, Hamlin N, Holroyd S, Hornsby T, Jagels K, Lacroix C, Maclean J, Moule S, Murphy L, Oliver K, Quail MA, Rajandream MA, Rutherford KM, Rutter S, Seeger K, Simon S, Simmonds M, Skelton J, Squares R, Squares S, Stevens K, Taylor K, Whitehead S, Woodward JR, Barrell BG. 2001. Massive gene decay in the leprosy bacillus. Nature 409:1007–1011. https://doi.org/10.1038/35059006.

14. Das C, Ghosh TS, Mande SS. 2011. Computational analysis of the ESX-1 region of Mycobacterium tuberculosis: insights into the mechanism of type VII secretion system. PLoS One 6:e27980. https://doi.org/10.1371/journal.pone.0027980.

15. Inwald J, Jahans K, Hewinson RG, Gordon SV. 2003. Inactivation of the Mycobacterium bovis homologue of the polymorphic RD1 gene Rv3879c (Mb3909c) does not affect virulence. Tuberculosis (Edinb) 83:387–393. https://doi.org/10.1016/j.tube.2003.08.018.

16. Bold TD, Davis DC, Penberthy KK, Cox LM, Ernst JD, de Jong BC. 2012. Impaired fitness of Mycobacterium africanum despite secretion of ESAT-6. J Infect Dis 205:984–990. https://doi.org/10.1093/infdis/jir883.

17. Ca B, Fonseca KL, Sousa J, Maceiras AR, Machado D, Sanca L, Rabna P, Rodrigues PNS, Viveiros M, Saraiva M. 2019. Experimental evidence for limited in vivo virulence of Mycobacterium africanum. Front Microbiol 10:2102. https://doi.org/10.3389/fmicb.2019.02102.

18. Kapopoulou A, Lew JM, Cole ST. 2011. The MycoBrowser portal: a comprehensive and manually annotated resource for mycobacterial genomes. Tuberculosis (Edinb) 91:8–13. https://doi.org/10.1016/j.tube.2010.09.006.

19. Stinear TP, Seemann T, Harrison PF, Jenkin GA, Davies JK, Johnson PD, Abdellah Z, Arrowsmith C, Chillingworth T, Churcher C, Clarke K, Cronin A, Davis P, Goodhead I, Holroyd N, Jagels K, Lord A, Moule S, Mungall K, Norbertczak H, Quail MA, Rabbinowitsch E, Walker D, White B, Whitehead S, Small PL, Brosch R, Ramakrishnan L, Fischbach MA, Parkhill J, Cole ST. 2008. Insights from the complete genome sequence of Mycobacterium marinum on the evolution of Mycobacterium tuberculosis. Genome Res 18:729–741. https://doi.org/10.1101/gr.075069.107.

20. Sani M, Houben EN, Geurtsen J, Pierson J, de Punder K, van Zon M, Wever B, Piersma SR, Jimenez CR, Daffe M, Appelmelk BJ, Bitter W, van der Wel N, Peters PJ. 2010. Direct visualization by cryo-EM of the mycobacterial capsular layer: a labile structure containing ESX-1-secreted proteins. PLoS Pathog 6:e1000794. https://doi.org/10.1371/journal.ppat.1000794.

21. Bosserman RE, Nicholson KR, Champion MM, Champion PA. 2019. A new ESX-1 substrate in Mycobacterium marinum that is required for hemolysis but not host cell lysis. J Bacteriol 201:e00760-18. https://doi.org/10.1128/JB.00760-18.

22. Champion MM, Williams EA, Pinapati RS, Champion PA. 2014. Correlation of phenotypic profiles using targeted proteomics identifies mycobacterial esx-1 substrates. J Proteome Res 13:5151–5164. https://doi.org/10.1021/pr500484w.

23. Gao LY, Guo S, McLaughlin B, Morisaki H, Engel JN, Brown EJ. 2004. A mycobacterial virulence gene cluster extending RD1 is required for cytolysis, bacterial spreading and ESAT-6 secretion. Mol Microbiol 53:1677–1693. https://doi.org/10.1111/j.1365-2958.2004.04261.x.

24. McLaughlin B, Chon JS, MacGurn JA, Carlsson F, Cheng TL, Cox JS, Brown EJ. 2007. A mycobacterium ESX-1-secreted virulence factor with unique requirements for export. PLoS Pathog 3:e105. https://doi.org/10.1371/journal.ppat.0030105.

25. Lienard J, Nobs E, Lovins V, Movert E, Valfridsson C, Carlsson F. 2020. The Mycobacterium marinum ESX-1 system mediates phagosomal permeabilization and type I interferon production via separable mechanisms. Proc Natl Acad Sci U S A 117:1160–1166. https://doi.org/10.1073/pnas.1911646117.

26. Parkash O, Pandey R, Kumar A, Kumar A. 2007. Performance of recombinant ESAT-6 antigen (ML0049) for detection of leprosy patients. Lett Appl Microbiol 44:524–530. https://doi.org/10.1111/j.1472-765X.2006.02099.x.

27. Spencer JS, Kim HJ, Marques AM, Gonzalez-Juarerro M, Lima MC, Vissa VD, Truman RW, Gennaro ML, Cho SN, Cole ST, Brennan PJ. 2004. Comparative analysis of B- and T-cell epitopes of Mycobacterium leprae and Mycobacterium tuberculosis culture filtrate protein 10. Infect Immun 72:3161–3170. https://doi.org/10.1128/IAI.72.6.3161-3170.2004.

28. Spencer JS, Marques MA, Lima MC, Junqueira-Kipnis AP, Gregory BC, Truman RW, Brennan PJ. 2002. Antigenic specificity of the Mycobacterium leprae homologue of ESAT-6. Infect Immun 70:1010–1013. https://doi.org/10.1128/IAI.70.2.1010-1013.2002.

29. van der Wel N, Hava D, Houben D, Fluitsma D, van Zon M, Pierson J, Brenner M, Peters PJ. 2007. M. tuberculosis and M. leprae translocate from the phagolysosome to the cytosol in myeloid cells. Cell 129:1287–1298. https://doi.org/10.1016/j.cell.2007.05.059.

30. Dhar N, McKinney JD. 2010. Mycobacterium tuberculosis persistence mutants identified by screening in isoniazid-treated mice. Proc Natl Acad Sci U S A 107:12275–12280. https://doi.org/10.1073/pnas.1003219107.

31. Chen JM, Boy-Rottger S, Dhar N, Sweeney N, Buxton RS, Pojer F, Rosenkrands I, Cole ST. 2012. EspD is critical for the virulence-mediating ESX-1 secretion system in Mycobacterium tuberculosis. J Bacteriol 194:884–893. https://doi.org/10.1128/JB.06417-11.

32. Drever K, Lim ZL, Zriba S, Chen JM. 2021. Protein synthesis and degradation inhibitors potently block Mycobacterium tuberculosis type-7 secretion system ESX-1 activity. ACS Infect Dis 7:273–280. https://doi.org/10.1021/acsinfecdis.0c00741.

33. Ligon LS, Hayden JD, Braunstein M. 2012. The ins and outs of Mycobacterium tuberculosis protein export. Tuberculosis (Edinb) 92:121–132. https://doi.org/10.1016/j.tube.2011.11.005.

34. Hickey TB, Thorson LM, Speert DP, Daffé M, Stokes RW. 2009. Mycobacterium tuberculosis Cpn60.2 and DnaK are located on the bacterial surface, where Cpn60.2 facilitates efficient bacterial association with macrophages. Infect Immun 77:3389–3401. https://doi.org/10.1128/IAI.00143-09.

35. Chen JM, Zhang M, Rybniker J, Basterra L, Dhar N, Tischler AD, Pojer F, Cole ST. 2013. Phenotypic profiling of Mycobacterium tuberculosis EspA point mutants reveals that blockage of ESAT-6 and CFP-10 secretion in vitro does not always correlate with attenuation of virulence. J Bacteriol 195:5421–5430. https://doi.org/10.1128/JB.00967-13.

36. Hirschfield GR, McNeil M, Brennan PJ. 1990. Peptidoglycan-associated polypeptides of Mycobacterium tuberculosis. J Bacteriol 172:1005–1013. https://doi.org/10.1128/jb.172.2.1005-1013.1990.

37. Lee BY, Hefta SA, Brennan PJ. 1992. Characterization of the major membrane protein of virulent Mycobacterium tuberculosis. Infect Immun 60:2066–2074. https://doi.org/10.1128/iai.60.5.2066-2074.1992.

38. Lucas M, Ryan JM, Watkins J, Early K, Kruh-Garcia NA, Mehaffy C, Dobos KM. 2021. Extraction and separation of mycobacterial proteins, p 77–107. In Parish T, Kumar A (ed), Mycobacteria protocols. Springer US, New York, NY.

39. Sharma D, Bose A, Shakila H, Das TK, Tyagi JS, Ramanathan VD. 2006. Expression of mycobacterial cell division protein, FtsZ, and dormancy proteins, DevR and Acr, within lung granulomas throughout guinea pig infection. FEMS Immunol Med Microbiol 48:329–336. https://doi.org/10.1111/j.1574-695X.2006.00160.x.

40. Brodin P, de Jonge MI, Majlessi L, Leclerc C, Nilges M, Cole ST, Brosch R. 2005. Functional analysis of early secreted antigenic target-6, the dominant T-cell antigen of Mycobacterium tuberculosis, reveals key residues involved in secretion, complex formation, virulence, and immunogenicity. J Biol Chem 280:33953–33959. https://doi.org/10.1074/jbc.M503515200.

41. Raffetseder J, Iakobachvili N, Loitto V, Peters PJ, Lerm M. 2019. Retention of EsxA in the capsule-like layer of Mycobacterium tuberculosis is associated with cytotoxicity and is counteracted by lung surfactant. Infect Immun 87:e00803-18. https://doi.org/10.1128/IAI.00803-18.

42. Singh P, Cole ST. 2011. Mycobacterium leprae: genes, pseudogenes and genetic diversity. Future Microbiol 6:57–71. https://doi.org/10.2217/fmb.10.153.

43. Daffé M, Marrakchi H. 2019. Unraveling the structure of the mycobacterial envelope. Microbiol Spectr. https://doi.org/10.1128/microbiolspec.GPP3-0027-2018.

44. Chirakos AE, Balaram A, Conrad W, Champion PA. 2020. Modeling tubercular ESX-1 secretion using Mycobacterium marinum. Microbiol Mol Biol Rev 84:e00082-19. https://doi.org/10.1128/MMBR.00082-19.

45. Corpet F. 1988. Multiple sequence alignment with hierarchical clustering. Nucleic Acids Res 16:10881–10890. https://doi.org/10.1093/nar/16.22.10881.

46. Bottai D, Majlessi L, Simeone R, Frigui W, Laurent C, Lenormand P, Chen J, Rosenkrands I, Huerre M, Leclerc C, Cole ST, Brosch R. 2011. ESAT-6 secretion-independent impact of ESX-1 genes espF and espG1 on virulence of Mycobacterium tuberculosis. J Infect Dis 203:1155–1164. https://doi.org/10.1093/infdis/jiq089.

47. Kim JK, Silwal P, Jo EK. 2020. Host-pathogen dialogues in autophagy, apoptosis, and necrosis during mycobacterial infection. Immune Netw 20:e37. https://doi.org/10.4110/in.2020.20.e37.

48. Mohareer K, Asalla S, Banerjee S. 2018. Cell death at the cross roads of host-pathogen interaction in Mycobacterium tuberculosis infection. Tuberculosis (Edinb) 113:99–121. https://doi.org/10.1016/j.tube.2018.09.007.

49. Wiens KE, Ernst JD. 2016. Type I interferon is pathogenic during chronic Mycobacterium africanum infection. J Infect Dis 214:1893–1896. https://doi.org/10.1093/infdis/jiw519.

50. Wiens KE, Ernst JD. 2016. The mechanism for type I interferon induction by Mycobacterium tuberculosis is bacterial strain-dependent. PLoS Pathog 12:e1005809. https://doi.org/10.1371/journal.ppat.1005809.

51. Wassermann R, Gulen MF, Sala C, Perin SG, Lou Y, Rybniker J, Schmid-Burgk JL, Schmidt T, Hornung V, Cole ST, Ablasser A. 2015. Mycobacterium tuberculosis differentially activates cGAS- and inflammasome-dependent intracellular immune responses through ESX-1. Cell Host Microbe 17:799–810. https://doi.org/10.1016/j.chom.2015.05.003.

52. Wong KW. 2017. The role of ESX-1 in Mycobacterium tuberculosis pathogenesis. Microbiol Spectr. https://doi.org/10.1128/microbiolspec.TBTB2-0001-2015.

53. Malhotra A. 2009. Tagging for protein expression. Methods Enzymol 463:239–258. https://doi.org/10.1016/S0076-6879(09)63016-0.

54. Zhang M, Chen JM, Sala C, Rybniker J, Dhar N, Cole ST. 2014. EspI regulates the ESX-1 secretion system in response to ATP levels in Mycobacterium tuberculosis. Mol Microbiol 93:1057–1065. https://doi.org/10.1111/mmi.12718.

55. Rybniker J, Chen JM, Sala C, Hartkoorn RC, Vocat A, Benjak A, Boy-Rottger S, Zhang M, Szekely R, Greff Z, Orfi L, Szabadkai I, Pato J, Keri G, Cole ST. 2014. Anticytolytic screen identifies inhibitors of mycobacterial virulence protein secretion. Cell Host Microbe 16:538–548. https://doi.org/10.1016/j.chom.2014.09.008.